

Modeling the typhoon disturbance effect on ecosystem carbon storage dynamics in a subtropical forest of China's coastal region

Jiaye Ping^{a,b}, Jian Zhou^{a,b}, Kun Huang^{a,b,c,*}, Xiaoying Sun^{a,b}, Huanfa Sun^{a,b}, Jianyang Xia^{a,b}

^a Zhejiang Tiantong Forest Ecosystem National Observation and Research Station, State Key Laboratory of Estuarine and Coastal Research, School of Ecological and Environmental Sciences, East China Normal University, Shanghai 200241, China

^b Research Center for Global Change and Ecological Forecasting, East China Normal University, Shanghai 200241, China

^c Institute of Eco-Chongming (IEC), East China Normal University, Shanghai, China

ARTICLE INFO

Keywords:

Carbon dynamics
Climate change
Extreme events
Forest equilibrium state

ABSTRACT

As an important ecological factor shaping terrestrial ecosystem states and destabilizing coastal forest ecosystems, typhoon events have become the focus of attention in recent years. However, there are limited studies on the change of carbon storage dynamics of subtropical forest ecosystems under typhoon disturbance. Here, we developed a theoretical ecosystem carbon cycle model combined with forest inventory data and measurements to evaluate pluriannual typhoon response of East Monsoon subtropical forest ecosystem carbon storage dynamics in Tiantong mountain (29°48'N, 121°47'E). We focused on the relationships between typhoon regime and ecosystem carbon storage dynamics, and forest resistance and resilience to typhoon disturbances. We showed that the disturbed plant biomass contributed to the reduced forest ecosystem carbon storage capacity. The modeling analyses underscored the critical role of biomass turnover time in forest ecosystem carbon storage capacity. The soil organic matter was highly stable under severe typhoons while the resistance of biomass and litter carbon amounts to increasingly severe typhoons decreased. The theoretical estimates provided by this study are instructive for the policy making of subtropical forest conservation and management under global environmental changes.

1. Introduction

Forests act as a large carbon sink to take in ~33% of the anthropogenic CO₂ emissions (Pan et al., 2011) and account for about 45% of the land carbon sink (Bonan, 2008). Tropical and subtropical forests contribute to about 70% of the global forest carbon sink (Pan et al., 2011; Suarez et al., 2019). Subtropical forests are largely located in the East Asian monsoon region, and the eddy covariance observations suggest the total net ecosystem productivity (NEP) of this region accounts for 8% of global forest NEP (Yu et al., 2014). The East Asian monsoon subtropical forests under increasing atmospheric nitrogen (N) deposition are expected to be a large carbon sink (Cui et al., 2019; Qiao et al., 2020). Therefore, understanding the carbon storage dynamics of East Asian monsoon subtropical forests is crucial for land-atmosphere carbon exchange predictions and climate mitigation in the future.

Forests, with large biomass carbon stocks, are vulnerable to the impact of strong winds such as typhoons (Reichstein et al., 2013). Large defoliations, branch stripping and even uprooting are the most common

effects of typhoon on the forest ecosystem (Lin et al., 2010). In the East Asian monsoon subtropical regions, forest structure and function of the coastal region have been threatened by typhoons. In the past decades, increasingly intensified landfalling typhoons have struck the forests of subtropical coastal region (Marois and Mitsch, 2015). For example, typhoon has dominated temporal fluctuations of litterfall mass in a subtropical forest in a 21-years field measurement (Lin et al., 2017). The magnitudes of NEP responses to typhoons are greatly affected due to the defoliation resulted from strong wind and intensive rainfall (Chen et al., 2014). Typhoon-induced foliage losses can decline forest aboveground biomass (Lin et al., 2017). Biomass turnover time, a proxy of tree longevity at ecosystem level, plays a crucial role in plant growth dynamics, and contributes to the feedback between the carbon cycle and climate (Erb et al., 2016). It measures how fast carbon will be released from biomass pool and is critical in regulating the carbon storage capacity (Wang et al., 2021). As a key variable property of ecosystem, biomass turnover time plays an important role in linking key processes in carbon cycle of forests (Malhi, 2012) and varies with precipitation,

* Corresponding author: School of Ecological and Environmental Sciences, East China Normal University, 500 Dongchuan Road, Shanghai 200241, China.
E-mail address: khuang@des.ecnu.edu.cn (K. Huang).

Table 1

A summary of typhoons directly hit coastal subtropical forests in China in 2012–2015.

Year	Name	Landing time	Landing wind speed	Interval time between two typhoons for the given year
2012	1209 Saola	2, Aug. 3:15	40 m/s	9 day
	1210 Damrey	2, Aug. 21:30	35 m/s	< 1 day
	1211 Haikui*	8, Aug. 3:20	42 m/s	5 day
	1307 Soulik	13, July 3:00	42 m/s	11 day
2013	1308 Cimaron	18, July 20:30	23 m/s	5 day
	1312 Trami	22, Aug. 2:40	35 m/s	34 day
	1319 Usagi	22, Sept. 19:40	45 m/s	31 day
	1323 Fitow	7, Oct. 1:15	42 m/s	14 day
	1407 Hagibis	15, June 16:50	23 m/s	5 day
2014	1410 Matmo	23, July 0:15	40 m/s	37 day
	1416 Fung- wong*	21, Sept. 10:00	28 m/s	60 day
	1509 Chan- Hom*	11, July 16:40	45 m/s	18 day
	1513 Soudelor	8, Aug. 4:40	50 m/s	27 day
2015	1521 Dujan	28, Sept. 17:50	48 m/s	51 day

Data credit: National Meteorological Center of China Meteorology Agency (NMC—CMA).

*Typhoons that directly affected the study site.

fire and other natural and anthropogenic disturbances (Carvalho et al., 2014).

Given the large carbon uptake by subtropical forests, how the internal ecosystem properties and typhoon characteristics jointly affect the forest carbon storage dynamics remain unclear. There are growing concerns and studies about the intensifying forest disturbance regimes, which pose a great risk to forest ecosystem services due to the disturbed forest carbon storage (Metsaranta et al., 2010; Seidl et al., 2014, 2018). Here, we estimate the long-term typhoon impacts on subtropical forest ecosystem carbon storage dynamics by modeling ecosystem properties and typhoon characteristics. The ecosystem is represented by a three-pool carbon cycle model (Weng et al., 2012), and the typhoon disturbance regime is characterized by the average severity and frequency.

The responses of ecosystem function to typhoon disturbance have been generally described by resistance and resilience (Chang et al., 2018). These two components consider concurrent and delayed effects of disturbances on ecosystem (Huang and Xia, 2019). Resistance quantifies the capacity to maintain its original level during the disturbance, and resilience describes the rate of ecosystem function recovering to its normal state after disturbance. The Tiantong forest site is located in the subtropical coastal region, and is frequently struck by typhoons (Table 1). Using the 4-year (2012–2015) litterfall measurements and forest inventory data at the Tiantong site, we adopt an ecosystem carbon cycle model to represent the ecosystem carbon processes, and a typhoon disturbance regime to characterize the typhoon severity and frequency. Thus, the derived analytical solution from the integration of the typhoon processes with the ecosystem carbon dynamics pattern is to examine the typhoon effect on the ecosystem carbon storage dynamics. With the field measurements and simulation experiments at the Tiantong subtropical forest site, this study aims to explore the following three issues: (a) relationships between typhoon regime and ecosystem carbon storage

dynamics; (b) role of biomass turnover time in typhoon disturbance affecting the ecosystem carbon storage capacity; and (c) resistance and resilience of ecosystem carbon storage dynamics to typhoon disturbances under various severity scenarios.

2. Material and methods

2.1. Site description

Tiantong mountain (29°48'N, 121°47'E) is located in low hilly areas in the most eastern central subtropical zone of Zhejiang province in China, with much forest vegetation well preserved. The average annual temperature and annual mean precipitation is 16.2 °C and 1374.7 mm, respectively (Qiao et al., 2020).

The elevation of this site is approximately 300 m, ranging from 304.3 to 602.9 m. The Tiantong forest site is about 12 ~ 15 km away from the east coastline of China and is frequently affected by typhoons (Table 1). Thus, it is an ideal place for evaluating the effect of typhoons on the dynamics of evergreen broadleaf forests (EBFs). The dominant species are *Castanopsis fargesii*, *Schima superba*, *Cyclobalanopsis sessilifolia*, *Eurya loquaiana* and *Litsea elongata*, subjected to the humid and warm climate. The frequent typhoon disturbance is a great concern for ecosystem dynamics, especially for litterfall (fallen leaves and twigs) dynamics (Sato et al., 2010) and nutrient cycling responses to typhoons (Wang et al., 2015; Xu et al., 2004).

2.2. Empirical results from field study experiment

2.2.1. Forest inventory

The inventory was conducted in a 20-ha permanent plot of the Tiantong mountain (Fig. S1) every five years. This plot is a rectangle with 500 m long from east to west and 400 m wide from south to north, one of the components of the Forest Global Earth Observatory (Forest-GEO) network (<https://forestgeo.si.edu/>). It is composed of 500 quadrats each 20 m × 20 m in size by setting stone piles at every 20 m, which were further divided into 16 subplots of 5 m × 5 m (Qiao et al., 2020). Two inventories of these subplots have been conducted in 2010 and 2015, respectively. All woody plants with diameter ≥ 1 cm at breast height (DBH) were numbered and DBH measured as well as the species identification and coordinates recorded. For the inventory in 2010, 154 species were recorded. Mean DBH of each species ranged from 1.00 to 44.64 cm. The inventory conducted in 2015 recorded 159 species and the mean DBH ranged from 1.24 to 43.74 cm. Detailed DBH measurements for each species of the two inventories can be found in Table S1.

2.2.2. Litterfall collection

To monitor the temporal dynamics of litterfall, 187 collectors were uniformly placed in the 20-ha plot (Fig. S2) in August 2011, each with an average height of 0.6 m and a valid collection area of 0.5 m² (Fig. S3). Here we employed the litterfall measurements collected every half a month from January 2012 to December 2015. The litterfall collected was classified according to leaves, branches, flowers, barks, seed appendages and woody debris after drying at 65 °C in the oven for more than 48 h to a constant weight. All the weight of components from litterfall was recorded.

2.2.3. Soil heterotrophic respiration measurement

Heterotrophic respiration of soil was measured with trench method as described by Zhou et al. (Zhou et al., 2007). To be specific, three 0.65 m × 0.65 m quadrats were randomly set up in each subplot. A trench was dug at a depth of 0.8 m, at which depth there was little fine root distribution. The 2.5 mm-thick PVC plates clung to the wall of the trench. To allow water to flow, each plate had 120 evenly distributed 5 mm diameter holes, and was covered with a 400-mesh nylon net to prevent the external roots from growing in the quadrat. To minimize the disturbance of trenching, the trench was refilled according to the

Table 2
Summary of the model parameter and input/output.

	Description	Value	Unit
Parameter	η	Ratio of carbon transferred from litter to SOM pool	0.25 /
	τ_1	Biomass turnover time	35 year
	τ_2	Litter turnover time	7.1 year
	τ_3	SOM turnover time	27.3 year
	s	Fraction of biomass removed by a typhoon disturbance (0–1)	/ /
	λ	Mean typhoon interval time	/ year
	σ	Typhoon disturbance index: portion of biomass carbon removed by typhoon per unit time	/ kg C kg C ⁻¹ year ⁻¹
	D	diameter at breast height (DBH)	/ cm
	ρ	Wood density	/ g·cm ⁻³
	$S1$	Typhoon typhoons scenarios with severity level 1	30% /
	$S2$	Typhoon typhoons scenarios with severity level 2	60% /
	$S3$	Typhoon typhoons scenarios with severity level 3	90% /
	\bar{X}_n	Average C content during normal years that excluded typhoon years	/ kg C m ⁻²
	X_t	C content in the typhoon year	/ kg C m ⁻²
	X_{t+1}	C content in the post-typhoon year	/ kg C m ⁻²
Input	U	Ecosystem carbon input (NPP)	0.77 kg C m ⁻² year ⁻¹
Output	X_1	Biomass carbon pool	/ kg C m ⁻²
	X_2	Litter carbon pool	/ kg C m ⁻²
	X_3	Soil organic matter (SOM) carbon pool	/ kg C m ⁻²
	\bar{X}	Ecosystem carbon content at equilibrium state	/ kg C m ⁻²

original soil profile. The heterotrophic respiration was measured once or twice a month between 9:00 am and 14:00 pm, using an LI-8100 portable soil CO₂ flux system attached to the soil CO₂ flux chamber (LI-COR. Inc., Lincoln, NE, USA).

2.3. Parameter estimation from field data

We used the empirical results from the field experiments to estimate parameter values used in this study (See the summary in Table 2). We estimated the aboveground biomass (AGB) by a general and well-validated biomass allometric model (Pilli et al., 2006),

$$M = a \cdot D^b \quad (1)$$

where M is the AGB of an individual tree, D is the diameter at breast height (DBH). Parameter $a \approx 0.3\rho$, where ρ is wood density; parameter $b = 2.5$ were adopted from Pilli et al., (2006). To estimate the total biomass of a standing tree, we used the ratio of AGB to belowground biomass (BGB) of subtropical evergreen broadleaf forests (~4.39). This number was calculated based on the forest data from 984 sites across China (Li and Ren, 2004).

Each litterfall collector was placed in the center with a radius of 30 m, and the area of each plot that maximized the amount of valid litterfall is $900\pi\text{m}^2$. The annual total dry weight of litterfall (ATDW, leaves and branches included) of each collector was counted from the year 2012 to 2015. Based on the above data, the following parameters were obtained.

Net primary productivity (NPP) of plot i was estimated by the following equation:

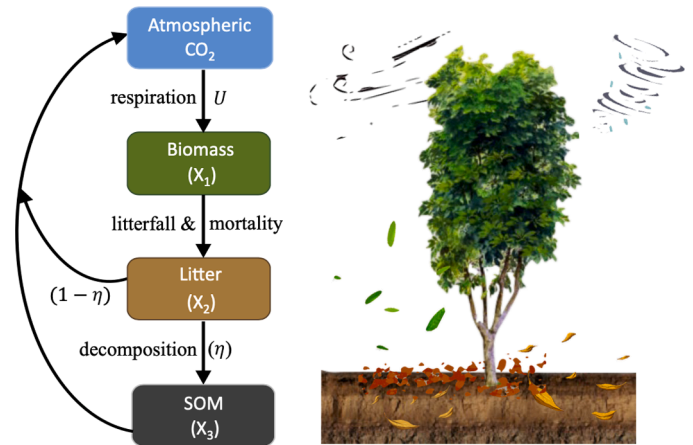


Fig. 1. Ecosystem C cycle model. Biomass (X_1), litter (X_2), and soil organic matter (SOM; X_3) are the three C pools. η is the fraction of C transferred to the SOM pool from the litter pool. U represents the net primary productivity (NPP). The autotrophic respiration is not shown here.

$$NPP_{aboveground, i} = (AGB_{2015, i} - AGB_{2010, i}) / 5 \quad (2)$$

where $AGB_{2010, i}$, $AGB_{2015, i}$ were the aboveground biomass of the first and second inventory of plot i in 2010 and 2015, respectively.

For evergreen broadleaf forests, the partitioning coefficients of NPP on leaf, root, and wood are 0.249, 0.551 and 0.200, respectively (Xia et al., 2013), thus C influx of plot i was,

$$U_i = NPP_i = NPP_{aboveground, i} / 0.449 \quad (3)$$

Consequently, the forest C input (U) was estimated as:

$$U = \left(\sum_i U_i / S_i \right) / 187 \approx 0.711 \text{ kg C m}^{-2} \text{ year}^{-1} \quad (4)$$

where S_i is the area of plot i . We used the ratio of C stock divided by C flux as the approximation of turnover times (Zhou and Luo, 2008). That is, for each plot i ,

$$\tau_{1, i} = Biomass_{2015, i} / NPP_i \quad (5)$$

where $Biomass_{2015, i}$ is the C stock of plot i in 2015 inventory. According to the measurement data from Tiantong plot, the biomass of surface litter (SLB) was 2.589 kg m^{-2} , together with the AGB of the coarse wood debris (CWD) that obtained for each plot, then

$$\tau_{2, i} = (SLB \cdot 900\pi + AGB_{CWD, i}) / ATDW_i$$

where $\tau_{2, i}$ is the turnover time of litterfall in each plot i . The total surface litter from litterfall collectors (e.g., leaves and fine root) in each plot ($SLB \cdot 900\pi$), and the aboveground biomass of coarse wood debris ($AGB_{CWD, i}$) were the C stock of litter pool. The C flux of litter pool was the recorded average annual total dry weight of litterfall in each plot ($ATDW_i$). Then the parameter τ_1 and τ_2 were estimated as:

$$\tau_1 = \sum_i \tau_{1, i} / 187 \approx 35 \text{ year} \quad (6)$$

$$\tau_2 = \sum_i \tau_{2, i} / 187 \approx 7.1 \text{ year} \quad (7)$$

The turnover time τ_3 was calculated as the soil carbon inventory divided by the C outflux of the reservoir. The heterotrophic respiration rate of the soil of the Tiantong plot was about $476.8 \text{ g C m}^{-2} \text{ year}^{-1}$, and the content of soil organic carbon was about $13,000 \text{ g m}^{-2}$, so

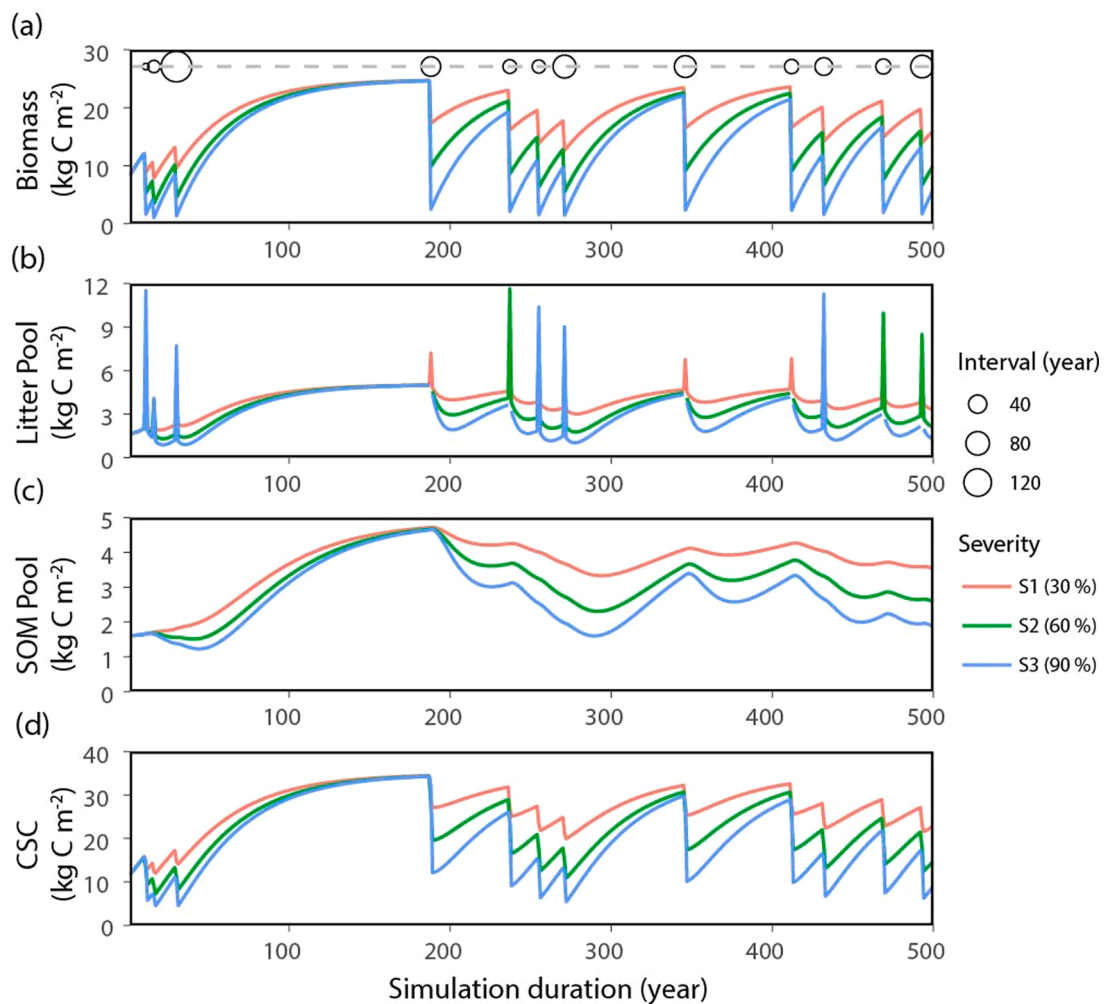


Fig. 2. The simulation of carbon amount dynamics of biomass (a), litter pool (b), SOM pool (c), and ecosystem carbon storage capacity (d). In each panel, the curves show the C storage dynamics under different typhoon severities in 500 years, respectively. S1, S2 and S3 represent three typhoon severities of 30%, 60% and 90%, of which the forest has been damaged, respectively. The magnitude of typhoon return interval, capturing the occurrence of typhoon as a Poisson process, is showed by the size of point in (a).

$\tau_3 \approx 27.3$ year. η is the C transfer coefficient from litter to SOM and set as 0.25 here (Hamilton et al., 2002; Weng et al., 2012).

2.4. Model description

In this section, a three-pool ecosystem carbon (C) cycle model, including the stand biomass, litter, and soil carbon pool, was adopted to represent the forest ecosystem C cycle (Fig. 1), and this scheme has been also used in modeling disturbance effects on ecosystem C dynamics by Weng et al., (2012). In this model, U stands for the C input, that is the net primary productivity (NPP), mainly supporting for the plant biomass growth. X_1 is the amount of C in the biomass pool with a C turnover time τ_1 . X_2 and X_3 are the C content of the litter pool and soil organic matter (SOM) with the C turnover time of τ_2 and τ_3 , respectively (Weng et al., 2012). Litter pool is consisted of the dead plant and litterfalls, part of which is released to the atmosphere by heterotrophic respiration and part of which is stabilized to become SOM. SOM would be broken down slowly by microbial respiration, released into air as CO_2 .

Typhoon or other wind storms affect forest ecosystem C storage dynamics by the intensification of litterfall, leading to an increasing size of litter C pools. The fraction of C content transferred from living biomass pools to litter pools largely depend on the wind severity. Here we introduce how typhoon disturbances are modeled and how the forest

ecosystem C storage dynamic process responds to typhoons.

According to previous studies about the disturbance characteristics (Smithwick et al., 2006), we assume typhoon disturbance are Poisson events and thus the typhoon regime is defined as the mean typhoon return interval (λ : a parameter of Poisson distribution), the mean severity of typhoon effects on forest biomass (s : low, moderate, or high levels of removal of carbon from biomass pool), and the probability density function of s . The probability of a typhoon happened in a given year is thus defined as $P(\text{typhoon}) = 1/\lambda$, and the distribution of intervals between two consequential typhoons is:

$$f(T, \lambda) = (1/\lambda) \cdot \exp(-T/\lambda) \tag{8}$$

where T is the interval between two consecutive typhoon disturbance events.

The severity, defined as the fraction of biomass removed by typhoons, ranges from 0 to 1 from the first principles. For typhoon, s is normally much lower than 1.

Following the mathematical derivations in Weng et al. (2012), the expectation of plant biomass X_1 in a disturbance regime, which is defined by λ and s , is

$$\bar{X}_1 = U\tau_1 \cdot \lambda / (\lambda + s\tau_1) \tag{9}$$

with the assumption of constant carbon input (U) and turnover rate (τ_1), which define a recovery pattern as $U\tau_1(1 - \exp(-t/\tau_1))$. The carbon content that was reduced from the biomass C pool due to typhoon disturbance was delivered to the litter pool at the same time. The default turnover rate of the biomass pool was $1/\tau_1$.

At equilibrium state, the total litter input equals NPP, so the major impact of typhoon on ecosystem C cycling was that it moved C from the biomass pool to the litter pool. The C storage of litter pool equals the product of C input and turnover time of litter pool:

$$\bar{X}_2 = U\tau_2 \quad (10)$$

And the expectation of soil pool C is $\bar{X}_3 = \eta U\tau_3$, where η is the transfer ratio from litters to SOM. Thus, the C storage capacity of forest ecosystem represented by the conceptual model (Fig. 1) at equilibrium state can be written as:

$$\bar{X} = U\tau_1 \cdot \lambda / (\lambda + s\tau_1) + U\tau_2 + \eta U\tau_3 \quad (11)$$

Considering the characteristics of typhoon, we defined a typhoon disturbance index, which was the portion of C amounts in biomass removed by typhoon per unit time, denoted as $\sigma = \bar{s} / \lambda$, where \bar{s} stands for the mean fraction of biomass removed by typhoons.

The ecosystem carbon storage capacity (CSC), same as defined by Luo et al. (2017), is the production of C input and the turnover time, that is,

$$CSC = NPP \times \text{turnover time} \quad (12)$$

The carbon storage capacity represents the maximum amount of carbon that an ecosystem can store under given environmental conditions for the specific year. Here it is used as an index to evaluate the capability of carbon sink for the subtropical forest ecosystem.

2.5. Forest resistance and resilience indicators

To clarify how shifts in typhoon disturbance will affect subtropical forest functions, the resistance and resilience as two indices were used to quantify the effects of typhoon on forest ecosystems (Huang and Xia, 2019). The resistance measures how stable a forest is to keep the C content during typhoon periods, while resilience describes the ability of forest to recover from the last typhoon (De Keersmaecker et al., 2015; van Ruijven and Berendse, 2010). Here we used the definition of resistance and resilience from Isbell et al. (2015), the two indices were calculated as follows,

$$\text{Resistance} = \frac{\bar{X}_n}{|X_t - \bar{X}_n|} \quad (13)$$

$$\text{Resilience} = \frac{|X_t - \bar{X}_n|}{|X_{t+1} - \bar{X}_n|} \quad (14)$$

where \bar{X}_n , X_t and X_{t+1} represent the average carbon amounts during normal years that excluded typhoon years, the C content in the year that typhoon happened, and that of the next year after a typhoon disturbance, respectively. These two indices are directly comparable for different C pools because they are unitless.

2.6. Typhoons scenarios setting

We designed three typhoon scenarios varying at severity levels and frequency. We used S1, S2 and S3 to represent three typhoon severities of 30%, 60% and 90%, of which the forest has been damaged, respectively. Mean typhoon return interval ranged from 0 to 120 years. These scenarios were implemented into the modeling approach to assess potential impacts of typhoon over long period of times (500 years) on ecosystem carbon fluxes, carbon storage capacity, resilience and resistance of forest ecosystem.

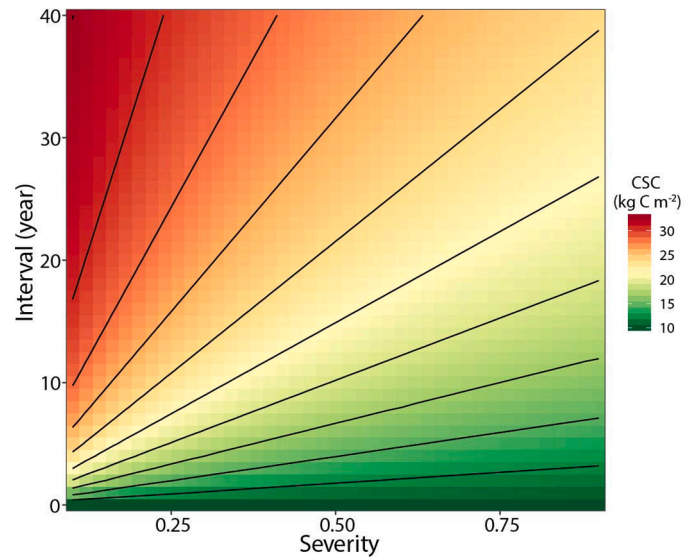


Fig. 3. Modeled carbon storage capacity with changes in typhoon severity and return interval. Axes are continuous gradients for typhoon severity (0–1) and return interval time (0–40 year). Estimated forest carbon storage capacity (surface with contour lines) is derived from the analytical solution (Eq. (11)).

3. Results

3.1. Relationships between typhoon regime and ecosystem carbon storage dynamics

Our simulations showed the different reductions of ecosystem carbon storage dynamics in response to enhanced typhoon disturbances indicated by three severity scenarios (Fig. 2). The losses of biomass pool and ecosystem carbon storage capacity (CSC) were reinforced with the increasing typhoon severities (Fig. 2a, d), and C amounts of the litter and SOM pool showed a quick and slight increase during the typhoon disturbances, respectively (Fig. 2b, c). During the 500-year simulation, the mean annual biomass pool for the S1 scenario was higher ($19.52 \text{ kg C m}^{-2}$) than the S2 scenario ($16.39 \text{ kg C m}^{-2}$) and S3 scenario ($14.02 \text{ kg C m}^{-2}$). For the SOM pool, it ranged from 2.73 kg C m^{-2} (S3) to 3.68 kg C m^{-2} (S1). The severer typhoon disturbance caused a decrease by 26.9% in the ecosystem CSC, when the typhoon severity varied from S1 (Severity = 0.3) to S3 (Severity = 0.9). Litter pool of the S3 scenario (3.13 kg C m^{-2}) exhibited lower than the moderate typhoon scenarios in the 500-year simulation.

Typhoon return intervals during the simulation were randomly set, and in our result, typhoon disturbance occurred 12 times (Fig. 2a). Although the litter pool for S3 scenario showed the largest increase during the 12 typhoon events, the annual mean litter pool for S3 scenario was lower than S1 (3.98 kg C m^{-2}) and S2 (3.46 kg C m^{-2}) scenarios. Compared with the annual mean pool size, the SOM pool during the typhoon events showed a minor decrease by 6% for S1 scenario, 6.1% for S2 scenario and 7% for S3 scenario, respectively.

In general, it is the frequency, instead of severity, that explains most of the variability in the different scenario tests (Fig. 3). The shorter the interval between typhoons, the higher the frequency of typhoons. In a range of severity, increasing typhoon frequency led to rapid changes in ecosystem CSC. For a certain frequency, the varied typhoon severities had similar effects on ecosystem CSC, that is, the severer the typhoon, the less CSC the ecosystem had. Shorter typhoon return interval impacted the recovery of the carbon storage after typhoon disturbances (< 40 years), and led to a decrease of ecosystem CSC (Fig. 3). The ecosystem carbon storage dynamics for each severity scenario showed similar recovery pattern under the various typhoon return intervals (Fig. 2). The forest ecosystem could store more carbon under longer

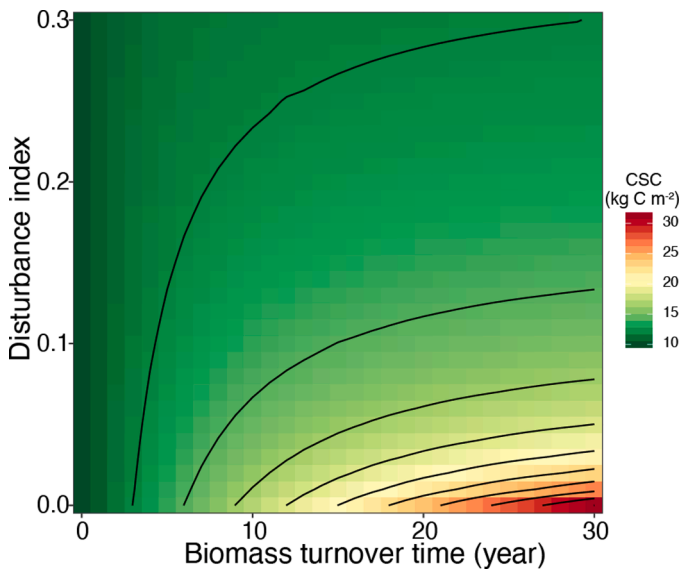


Fig. 4. Modeled ecosystem carbon storage capacity (CSC) with changes in biomass turnover time and disturbance index ($\sigma = s/\lambda$). Axes are continuous gradients for biomass turnover time (0 - 30 year) and disturbance index (0 - 0.3).

typhoon return intervals and less severe typhoons (Fig. 3).

3.2. Typhoon-induced variations of biomass turnover time and ecosystem carbon storage capacity

Forest ecosystem carbon storage dynamics modeled with a typhoon disturbance regime is determined by ecosystem properties (biomass turnover time affected by typhoon) on the one hand, and by typhoon characteristics (severity and frequency) on the other hand. The disturbance index was defined to describe the fraction of biomass carbon removed by typhoon per unit of time. Thus, this modeling approach evaluated the carbon storage at dynamic equilibrium states can be viewed as a function of ecosystem internal properties and typhoon

characteristics. The biomass turnover time was affected directly by the typhoon-induced defoliation, and we calculated the effects of typhoon disturbance (ratio of severity to interval) and biomass turnover time on forest ecosystem carbon storage capacity (Fig. 4). With moderate typhoon disturbance ($\sigma < 0.1 \pm 0.01$), the increasing biomass turnover time (i.e., less defoliation and slower carbon cycling rate) accelerated the ecosystem CSC (Fig. 4). Fig. 4 showed that the sensitivity of ecosystem carbon storage to typhoon was determined by the biomass turnover time affected by typhoons. Both internal ecosystem properties and disturbance characteristics contributed to the response of forest ecosystem carbon storage capacity to typhoons.

3.3. Modeled forest resistance and resilience to typhoon disturbances

The simulated typhoon resistance of biomass pool, litter pool and ecosystem CSC varied with severities, and the typhoon resistance of SOM pool showed no significant variations under increasingly severe typhoons (Fig. 5a). Typhoon resistance of biomass pool and litter pool was the most sensitive to the variations of typhoon severity. With the increasing typhoon severities, resistance of biomass pool was significantly reduced from 4.09 ± 1.9 for S1 scenario to 1.14 ± 0.04 for S3 scenario ($p < 0.001$). And the resistance of litter pool peaked at 2.81 ± 0.48 (S1 scenario), followed by 1.06 ± 0.35 (S2 scenario), and lastly by 0.46 ± 0.16 (S3 scenario). The typhoon resistance of ecosystem CSC showed statistical differences between the S1 scenario and S3 scenario ($p < 0.05$).

Our resilience simulations also revealed that the typhoon resilience of biomass pool, litter pool, SOM pool and ecosystem CSC did not show significant differences among the severity scenarios (Fig. 5b). This implied that resilience of the forest ecosystem carbon storage dynamics is insensitive to the variations of typhoon severities.

4. Discussion

4.1. Changes in biomass turnover time and ecosystem carbon storage capacity with varied typhoon regimes

Biomass turnover time, as a key parameter to determine carbon storage in forest ecosystems, is sensitive to precipitation, natural and

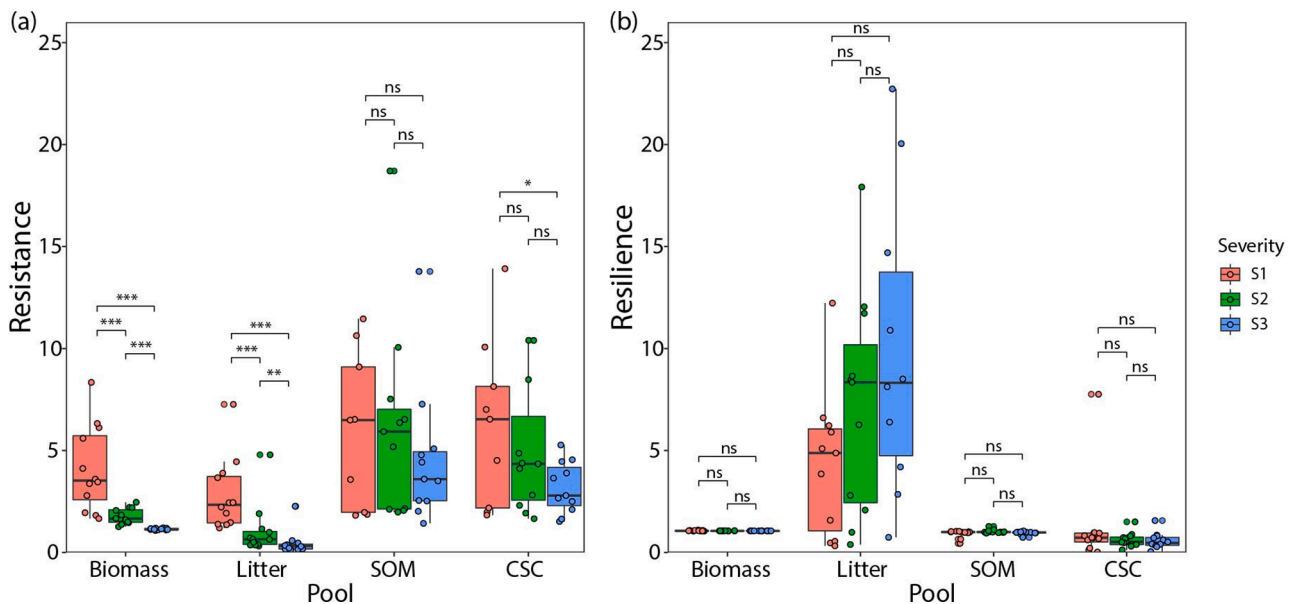


Fig. 5. The resistance (a) and resilience (b) of biomass pool, litter pool, SOM pool, and ecosystem CSC with three typhoon severities of 30% (S1), 60% (S2) and 90% (S3), respectively. The boxplots show the resistance and resilience of three carbon pools and CSC to the 12 simulated typhoon events for each severity scenario. The significance test is performed by a statistical test (*t*-test) to all pairwise comparisons under three severities for carbon pools and ecosystem CSC. The significance level is added onto each panel with *** ($p < 0.001$), ** ($p < 0.01$), * ($p < 0.05$) and ns (non-significant).

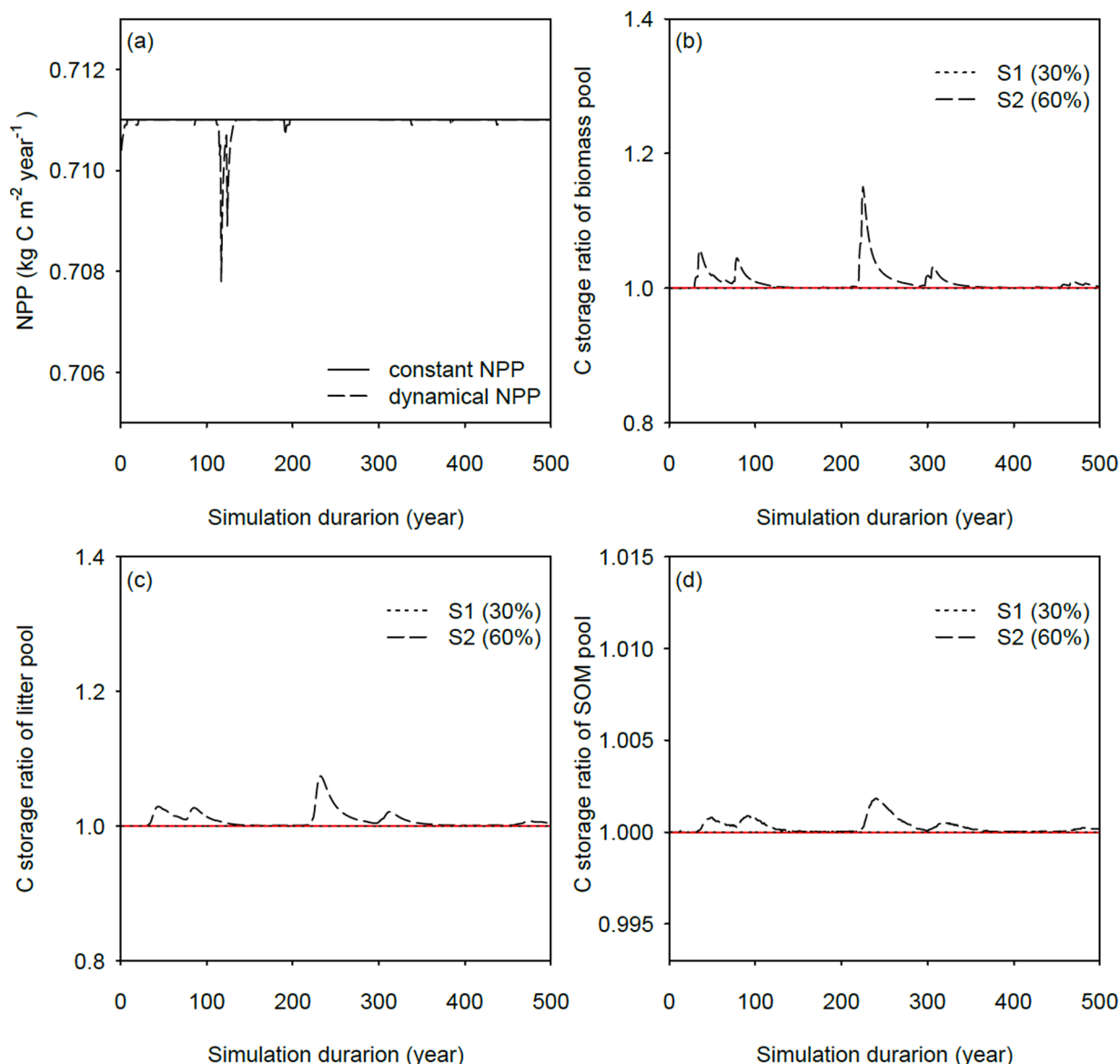


Fig. 6. Robustness analysis of carbon storage to the recovery patterns of NPP. (a) NPP patterns in two assumptions: constant and dynamical. (b) Ratios of simulated carbon storage in biomass pool at constant NPP to that at variable NPP. (c) and (d) are the same with (b) but for litter and soil, respectively. The red solid line is a reference line showing the ratio of 1. The dotted and dash lines in (b)-(d) indicate two typhoon severity level, S1 (30%) and S2 (60%), i.e., 30% and 60% of which the forest has been damaged, respectively. (For interpretation of the references to color in this figure legend, the reader is referred to the web version of this article.)

anthropogenic disturbances and management activities (Carvalhois et al., 2014; Erb et al., 2016). Changes in biomass turnover time and typhoon regime contribute to the forest ecosystem carbon storage dynamics under typhoon disturbance. Typhoon-induced defoliation and biomass losses could accelerate the rate of carbon turnover in the ecosystem carbon cycling, and finally lower the mean time that carbon atoms reside in the ecosystem (Xia et al., 2013). Part of the biomass losses are transformed to litterfall and coarse woody debris, and cause CO_2 emission to the atmosphere by the microbial activities (Luo et al., 2017; Xia et al., 2013). The reduced biomass turnover time caused by defoliation and branch fall thus influences the ecosystem carbon storage capacity (Fig. 4). Attentions should be paid to the role of ecosystem properties in response to typhoon.

4.2. Stabilization mechanism of ecosystem carbon storage dynamics under typhoon disturbances

Typhoon disturbance plays an important role in shaping the forest

ecosystem carbon storage dynamics of coastal regions. The result of typhoon resilience suggests that the subtropical forests are high resilient to the typhoon disturbance. Subtropical forests are capable of recovering from regular typhoon disturbance in one year (Lin et al., 2017). Biomass and litter pools are more likely to be disturbed by typhoon, explained by defoliated litters and tree mortality (Lin et al., 2020). Furthermore, evidences showed that wind disturbance was the dominant cause of the observed increase of large-trees mortality in this subtropical monsoon evergreen forest (Lu et al., 2021). Thus, typhoons do play a critical role in forest carbon dynamics in the subtropical forest of China's coastal region. While the SOM pool shows a high stability to typhoon disturbance (Fig. 5). Wind and rain are two typical forces for typhoon. We do not connect the impacts of typhoons to the view of hydrology, geomorphology and biogeochemistry in this study, for example, rainfall effect on soil respiration and carbon stored in the soil (Ryan and Law, 2005). These complex interactions and processes are beneficial to the understanding of forest recovery from typhoon regime.

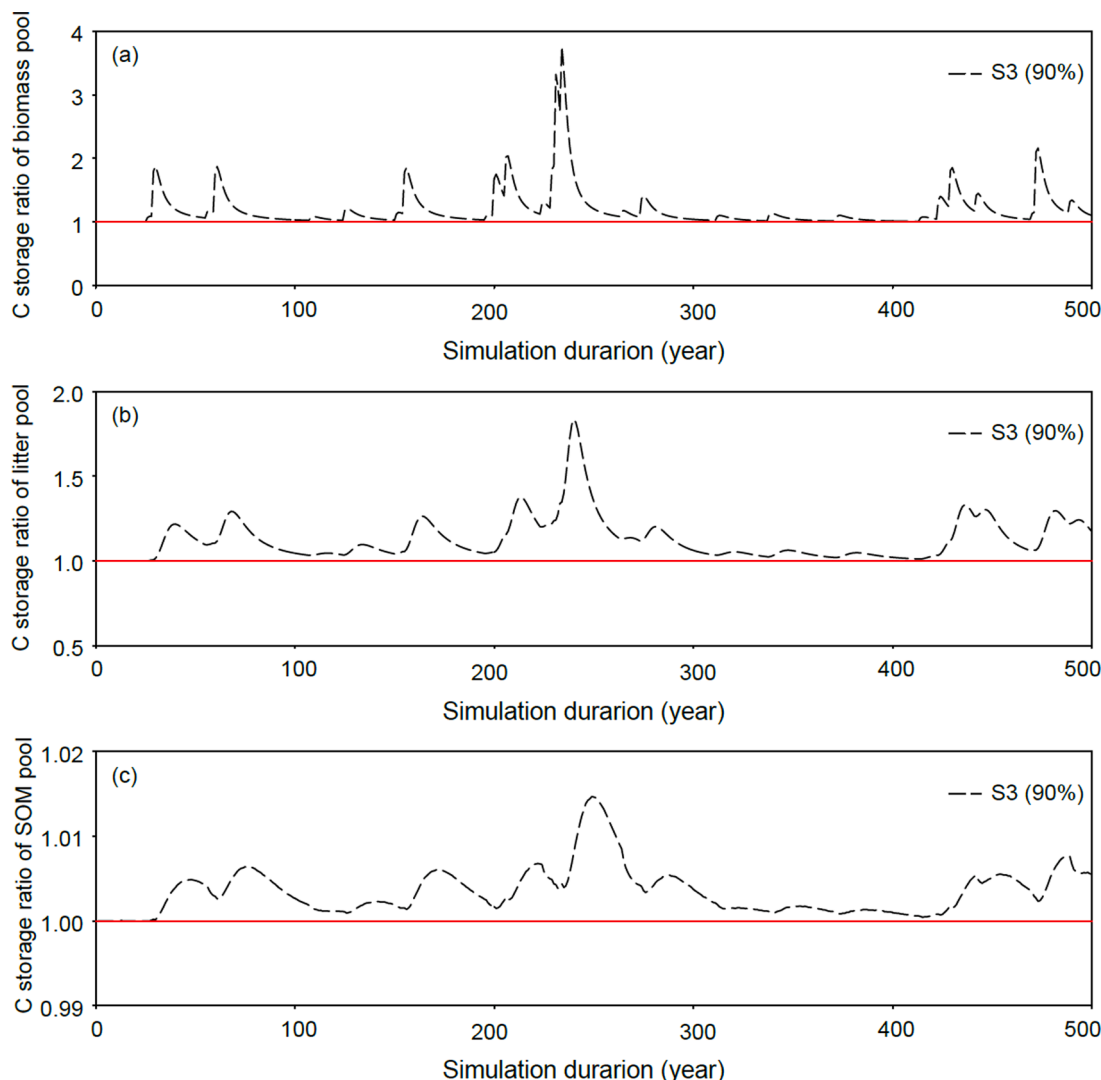


Fig. 7. Ratios of simulated carbon storage at constant NPP to that at variable NPP in biomass (a), litter (b), and SOM pool (c) with 90% of typhoon severity, respectively. The dashed line showed the ratio at S3 typhoon scenario. The red solid line indicated the reference line with ratio being 1. (For interpretation of the references to color in this figure legend, the reader is referred to the web version of this article.)

4.3. Robustness of the model performance

The robustness analyses show the uncertainties caused by the assumptions of the constant carbon input over time. We showed the NPP dynamics at constant NPP and that at variable NPP (Fig. 6a), generated based on a realistic NPP pattern (Weng et al., 2012). We also tested the biases for two typhoon scenarios with slight and moderate severity levels (Fig. 6b-d). The ratios of the simulated carbon content of the biomass, litter and SOM pool at two NPP patterns were closely equaling to 1. The SOM pool performed the best robust at two NPP patterns with the ratio less than 1.002. For the scenario of S1, the recovery pattern of all three carbon pools were identical at two NPP patterns. Thus, the uncertainties resulted from constant NPP were small over long period of times in the case of a mild or moderate typhoon severity which close to the actual situation.

4.4. Model limitation and uncertainty

There are uncertainties in modeling the overall impacts of typhoons on forest ecosystem carbon storage dynamics. Limited typhoon information may not be able to fully represent the long-term characteristics of typhoons, although typhoon data are collected to match the field

experimental data in this study. So, the results may vary with the severity and frequency of future typhoons sensitive to climate changes. The post-typhoon field surveys are needed to evaluate the modeling typhoon effects. It is cautious that although the model predicts the forest carbon storage at the dynamic equilibrium states, the modeling results are constrained from the data input. More details of ecosystem processes at the local scale are necessary to improve the model performance.

The assumption we used in the model, like the constant mineralization rate for the litter and SOM following first-order decay functions, would cause uncertainties due to the model structure (Xia et al., 2013). However, due to the stable soil organic matter and the lag effects to climate changes over long-time scales (Schmidt et al., 2011; Trumbore, 1997), this assumption can be viewed as an approximation in modeling approach.

Although we have shown the model performance is robust with slight and moderate severity levels (Fig. 6), attention must be paid to the uncertainty caused by the constant NPP assumption in the case of extremely strong typhoons. With typhoon severity up to 90%, most of the ratios of simulated carbon storage at constant NPP to that at variable NPP were off and above 1 (Fig. 7). In biomass pool, the maximum deviation is up to 3.76 times (Fig. 7a) and 1.83 in litter pool (Fig. 7b). However, it is noted that the SOM pool remained the best robust

performance with the maximum ratio less than 1.015 notably at 90% severity (Fig. 7c).

4.5. Implications

This study is an attempt to analyze the typhoon disturbance in influencing the forest ecosystem carbon storage by modeling experiments. Long-term ground measurements are strongly needed in the future to further investigate the potential mechanisms for the post-typhoon recovery of forest ecosystem function.

Forest disturbance regimes have been changing profoundly in recent years, with climate being a prominent driver of disturbance change (Seidl et al., 2014). Typhoon, whose frequency is to be increasing, is a common disturbance in subtropical forests (Lin et al., 2017). Modeling of typhoon disturbance effects on ecosystem carbon storage dynamic is insightful for understanding the role of subtropical forests of China's coastal region in global carbon cycle on the one hand, because the subtropical forest ecosystems in the East Asian monsoon region provide a large net carbon sink and figure prominently in the global carbon budget (Yu et al., 2014). The knowledge of typhoon effects on evergreen broadleaf forests (EBFs) is improved through this study, thus the instruction of conservations for subtropical forests. On the other hand, the typhoon regime study helps to improve the understanding of the link between forest carbon storage dynamics and disturbances under climate change and to provide reference for future forest development analysis.

In most Earth system models (ESMs), e.g., the Community Land Model 5.0 (CLM5.0), have comprehensive and explicit representations of the key biogeophysical and biogeochemical processes and disturbance regimes like fire. However, few ESMs have detailed processes of wind effects on terrestrial carbon cycle as an independent module, which implies the demand to establish a theoretical model to understand the carbon storage capacity of forests under typhoon disturbance. This work provides a perspective to understand the carbon storage capacity by models. Thus, the results acquired from this model can be used as an estimation tool for large-scale inversion and model initialization.

5. Conclusions

In summary, this study investigates an important topic in global change ecology as typhoon frequency is to be increasing with climate change, leading to uncertain impacts on the forest carbon cycling in South-East Asia, a region with significant carbon stocks. This study simulates typhoon response of subtropical forest ecosystem carbon storage dynamics based on an original experimental design and a conceptual ecosystem carbon cycle model, considering the typhoon disturbance regime. The results show both the internal ecosystem properties and disturbance regime contributed to the response of forest ecosystem carbon storage capacity to typhoons. Furthermore, typhoons influence the resistance of forest ecosystem carbon storage capacity primarily through biomass and litter carbon amounts whereas soil organic matter remains a high stability under typhoon disturbance over long period of times. Although the increasing severe typhoon disturbance threatens the structure and function of East Asian monsoon subtropical forests in the coastal regions, limiting the prediction in land-atmosphere carbon exchange and forest management for forest conservation, the results show the subtropical forests could be able to recover from regular typhoon disturbances even if typhoon frequency is to be increasing with climate change.

CRedit author statement

Jiaye Ping: Conceptualization, Methodology, Investigation, Data curation, Visualization, Writing - original draft.

Jian Zhou: Methodology

Kun Huang: Conceptualization, Methodology, Visualization, Writing - review & editing, Supervision, Funding acquisition.

Xiaoying Sun: Methodology, Data curation.

Huanfa Sun: Investigation, Resources.

Jiayang Xia: Conceptualization, Supervision, Writing - review & editing, Funding acquisition.

Declaration of Competing Interest

The authors declare that they have no known competing financial interests or personal relationships that could have appeared to influence the work reported in this paper.

Acknowledgements

This work was financially supported by the National Key R&D Program of China (2017YFA0604600), the National Natural Science Foundation of China (31800400, 41601099), and the Fundamental Research Funds for the Central Universities in China.

Supplementary materials

Supplementary material associated with this article can be found, in the online version, at doi:10.1016/j.ecolmodel.2021.109636.

References

- Bonan, G.B., 2008. Forests and climate change: forcings, feedbacks, and the climate benefits of forests. *Science* 320, 1444–1449.
- Carvalho, N., Forkel, M., Khomik, M., Bellarby, J., Jung, M., Migliavacca, M., Mu, M., Saatchi, S., Santoro, M., Thurner, M., Weber, U., Ahrens, B., Beer, C., Cescatti, A., Randerson, J.T., Reichstein, M., 2014. Global covariation of carbon turnover times with climate in terrestrial ecosystems. *Nature* 514, 213–217.
- Chang, C.-T., Vadeboncoeur, M.A., Lin, T.-C., 2018. Resistance and resilience of social-ecological systems to recurrent typhoon disturbance on a subtropical island: Taiwan. *Ecosphere* 9.
- Chen, H., Lu, W., Yan, G., Yang, S., Lin, G., 2014. Typhoons exert significant but differential impacts on net ecosystem carbon exchange of subtropical mangrove forests in China. *Biogeosciences* 11, 5323–5333.
- Cui, E., Huang, K., Arain, M.A., Fisher, J.B., Huntzinger, D.N., Ito, A., Luo, Y., Jain, A.K., Mao, J., Michalak, A.M., Niu, S., Parazoo, N.C., Peng, C., Peng, S., Poulter, B., Ricciuto, D.M., Schaefer, K.M., Schwalm, C.R., Shi, X., Tian, H., Wang, W., Wang, J., Wei, Y., Yan, E., Yan, L., Zeng, N., Zhu, Q., Xia, J., 2019. Vegetation functional properties determine uncertainty of simulated ecosystem productivity: a traceability analysis in the East Asian Monsoon Region. *Glob. Biogeochem. Cycles* 33, 668–689.
- De Keersmaecker, W., Lhermitte, S., Tits, L., Honnay, O., Somers, B., Coppin, P., 2015. A model quantifying global vegetation resistance and resilience to short-term climate anomalies and their relationship with vegetation cover. *Glob. Ecol. Biogeogr.* 24, 539–548.
- Erb, K.-H., Fetzel, T., Plutzer, C., Kastner, T., Lauk, C., Mayer, A., Niederschneider, M., Körner, C., Haberl, H., 2016. Biomass turnover time in terrestrial ecosystems halved by land use. *Nat. Geosci.* 9, 674–678.
- Hamilton, J.G., DeLucia, E.H., George, K., Naidu, S.L., Finzi, A.C., Schlesinger, W.H., 2002. Forest carbon balance under elevated CO₂. *Oecologia* 131, 250–260.
- Huang, K., Xia, J., 2019. High ecosystem stability of evergreen broadleaf forests under severe droughts. *Glob. Chang. Biol.* 25, 3494–3503.
- Isbell, F., Craven, D., Connolly, J., Loreau, M., Schmid, B., Beierkuhnlein, C., Bezemer, T.M., Bonin, C., Bruehlheide, H., de Luca, E., Ebeling, A., Griffin, J.N., Guo, Q., Hautier, Y., Hector, A., Jentsch, A., Kreyling, J., Lanta, V., Manning, P., Meyer, S.T., Mori, A.S., Naeem, S., Niklaus, P.A., Polley, H.W., Reich, P.B., Roscher, C., Seabloom, E.W., Smith, M.D., Thakur, M.P., Tilman, D., Tracy, B.F., van der Putten, W.H., van Ruijven, J., Weigelt, A., Weisser, W.W., Wilsey, B., Eisenhauer, N., 2015. Biodiversity increases the resistance of ecosystem productivity to climate extremes. *Nature* 526, 574–U263.
- Li, G., Ren, H., 2004. Biomass and net primary productivity of the forests in different climatic zones of China. *Trop. Geogr.* 24 (4), 306–310.
- Lin, K.-C., Hamburg, S.P., Wang, L., Duh, C.-T., Huang, C.-M., Chang, C.-T., Lin, T.-C., 2017. Impacts of increasing typhoons on the structure and function of a subtropical forest: reflections of a changing climate. *Sci. Rep.* 7.
- Lin, T.-C., Hamburg, S.P., Lin, K.-C., Wang, L.-J., Chang, C.-T., Hsia, Y.-J., Vadeboncoeur, M.A., Mabry McMullen, C.M., Liu, C.-P., 2010. Typhoon disturbance and forest dynamics: lessons from a Northwest Pacific Subtropical Forest. *Ecosystems* 14, 127–143.
- Lin, T.-C., Hogan, J.A., Chang, C.-T., 2020. Tropical cyclone ecology: a scale-link perspective. *Trends Ecol. Evol.* (Amst.) 35, 594–604.
- Lu, R., Qiao, Y., Wang, J., Zhu, C., Cui, E., Xu, X., He, Y., Zhao, Z., Du, Y., Yan, L., Shen, G., Yang, Q., Wang, X., Xia, J., 2021. The U-shaped pattern of size-dependent mortality and its correlated factors in a subtropical monsoon evergreen forest. *J. Ecol.* 00, 1–13.

- Luo, Y., Shi, Z., Lu, X., Xia, J., Liang, J., Jiang, J., Wang, Y., Smith, M.J., Jiang, L., Ahlstrom, A., Chen, B., Hararuk, O., Hastings, A., Hoffman, F., Medlyn, B., Niu, S., Rasmussen, M., Todd-Brown, K., Wang, Y.-P., 2017. Transient dynamics of terrestrial carbon storage: mathematical foundation and its applications. *Biogeosciences* 14, 145–161.
- Maihi, Y., 2012. The productivity, metabolism and carbon cycle of tropical forest vegetation. *J. Ecol.* 100, 65–75.
- Marois, D.E., Mitsch, W.J., 2015. Coastal protection from tsunamis and cyclones provided by mangrove wetlands - a review. *Int. J. Biodivers. Sci. Ecosyst. Serv. Manage.* 11, 71–83.
- Metsaranta, J.M., Kurz, W.A., Neilson, E.T., Stinson, G., 2010. Implications of future disturbance regimes on the carbon balance of Canada's managed forest (2010-2100). *Tellus Ser. B-Chem. Phys. Meteorol.* 62, 719–728.
- Pan, Y., Birdsey, R.A., Fang, J., Houghton, R., Kauppi, P.E., Kurz, W.A., Phillips, O.L., Shvidenko, A., Lewis, S.L., Canadell, J.G., Ciais, P., Jackson, R.B., Pacala, S.W., McGuire, A.D., Piao, S., Rautiainen, A., Sitch, S., Hayes, D., 2011. A Large and Persistent Carbon Sink in the World's Forests. *Science* 333, 988–993.
- Pilli, R., Anfodillo, T., Carrer, M., 2006. Towards a functional and simplified allometry for estimating forest biomass. *For. Ecol. Manage.* 237, 583–593.
- Qiao, Y., Wang, J., Liu, H., Huang, K., Yang, Q., Lu, R., Yan, L., Wang, X., Xia, J., 2020. Depth-dependent soil C-N-P stoichiometry in a mature subtropical broadleaf forest. *Geoderma* 370.
- Reichstein, M., Bahn, M., Ciais, P., Frank, D., Mahecha, M.D., Seneviratne, S.I., Zscheischler, J., Beer, C., Buchmann, N., Frank, D.C., Papale, D., Rammig, A., Smith, P., Thonicke, K., van der Velde, M., Vicca, S., Walz, A., Wattenbach, M., 2013. Climate extremes and the carbon cycle. *Nature* 500, 287–295.
- Ryan, M.G., Law, B.E., 2005. Interpreting, measuring, and modeling soil respiration. *Biogeochemistry* 73, 3–27.
- Sato, T., Kominami, Y., Saito, S., Niyama, K., Tanouchi, H., Nagamatsu, D., Nomiya, H., 2010. Temporal dynamics and resilience of fine litterfall in relation to typhoon disturbances over 14 years in an old-growth lucidophyllous forest in southwestern Japan. *Plant. Ecol.* 208, 187–198.
- Schmidt, M.W.I., Torn, M.S., Abiven, S., Dittmar, T., Guggenberger, G., Janssens, I.A., Kleber, M., Koegel-Knabner, I., Lehmann, J., Manning, D.A.C., Nannipieri, P., Rasse, D.P., Weiner, S., Trumbore, S.E., 2011. Persistence of soil organic matter as an ecosystem property. *Nature* 478, 49–56.
- Seidl, R., Klöner, G., Rammer, W., Essl, F., Moreno, A., Neumann, M., Dullinger, S., 2018. Invasive alien pests threaten the carbon stored in Europe's forests. *Nat. Commun.* 9, 1626.
- Seidl, R., Schelhaas, M.J., Rammer, W., Verkerk, P.J., 2014. Increasing forest disturbances in Europe and their impact on carbon storage. *Nat. Clim. Chang.* 4, 806–810.
- Smithwick, E.A.H., Harmon, M.E., Domingo, J.B., 2006. Changing temporal patterns of forest carbon stores and net ecosystem carbon balance: the stand to landscape transformation. *Landsc. Ecol.* 22, 77–94.
- Suarez, D.R., Rozendaal, D.M.A., De Sy, V., Phillips, O.L., Alvarez-Davila, E., Anderson-Teixeira, K., Araujo-Murakami, A., Arroyo, L., Baker, T.R., Bongers, F., Brienen, R.J.W., Carter, S., Cook-Patton, S.C., Feldpausch, T.R., Griscom, B.W., Harris, N., Herault, B., Honorio Coronado, E.N., Leavitt, S.M., Lewis, S.L., Marimon, B.S., Monteagudo Mendoza, A., N'Dja, J.K., N'Guessan, A.E., Poorter, L., Qie, L., Rutishauser, E., Sist, P., Sonke, B., Sullivan, M.J.P., Vilanova, E., Wang, M.M.H., Martius, C., Herold, M., 2019. Estimating aboveground net biomass change for tropical and subtropical forests: refinement of IPCC default rates using forest plot data. *Glob. Chang. Biol.* 25, 3609–3624.
- Trumbore, S.E., 1997. Potential responses of soil organic carbon to global environmental change. *Proc. Natl. Acad. Sci. U.S.A.* 94, 8284–8291.
- van Ruijven, J., Berendse, F., 2010. Diversity enhances community recovery, but not resistance, after drought. *J. Ecol.* 98, 81–86.
- Wang, J., Li, W., Ciais, P., Ballantyne, A., Goll, D., Huang, X., Zhao, Z., Zhu, L., 2021. Changes in biomass turnover times in tropical forests and their environmental drivers from 2001 to 2012. *Earth's Future* 9.
- Wang, T., Liu, G., Gao, L., Zhu, L., Fu, Q., Li, D., 2015. Biological and nutrient responses to a typhoon in the yangtze estuary and the adjacent sea. *J. Coast. Res.* 32, 323–332.
- Weng, E., Luo, Y., Wang, W., Wang, H., Hayes, D.J., McGuire, A.D., Hastings, A., Schimel, D.S., 2012. Ecosystem carbon storage capacity as affected by disturbance regimes: a general theoretical model. *J. Geophys. Res.* 117.
- Xia, J., Luo, Y., Wang, Y.-P., Hararuk, O., 2013. Traceable components of terrestrial carbon storage capacity in biogeochemical models. *Glob. Chang. Biol.* 19, 2104–2116.
- Xu, X.N., Hirata, E., Shibata, H., 2004. Effect of typhoon disturbance on fine litterfall and related nutrient input in a subtropical forest on Okinawa Island., Japan. *Basic Appl. Ecol.* 5, 271–282.
- Yu, G., Chen, Z., Piao, S., Peng, C., Ciais, P., Wang, Q., Li, X., Zhu, X., 2014. High carbon dioxide uptake by subtropical forest ecosystems in the East Asian monsoon region. In: *Proceedings of the National Academy of Sciences of the United States of America*, 111, pp. 4910–4915.
- Zhou, T., Luo, Y., 2008. Spatial patterns of ecosystem carbon residence time and NPP-driven carbon uptake in the conterminous United States. *Glob. Biogeochem. Cycles* 22.
- Zhou, X., Wan, S., Luo, Y., 2007. Source components and interannual variability of soil CO₂ efflux under experimental warming and clipping in a grassland ecosystem. *Glob. Chang. Biol.* 13, 761–775.